



H₂ accumulation and N₂ fixation variation by Ni limitation in *Cyanothece*

Sing-how Tuo ¹, Irene B. Rodriguez,^{1,a} Tung-Yuan Ho ^{1,2*}

¹Research Center for Environmental Changes, Academia Sinica, Taipei, Taiwan

²Institute of Oceanography, National Taiwan University, Taipei, Taiwan

Abstract

Ni is an essential cofactor in NiFe-uptake hydrogenase, an enzyme regulating H₂ metabolism in diazotrophic cyanobacteria, the major H₂ producers in the surface ocean globally. Here, we investigated the effect of Ni supply on H₂ production and N₂ fixation by using a model marine cyanobacterial diazotroph, *Cyanothece*. By mediating total dissolved Ni concentrations from 100 to 0.03 nmol L⁻¹ in a trace metal-defined culture medium, we demonstrated that Ni deficiency results in H₂ accumulation, coupled with decreasing Ni quotas, growth rates, and occasionally relatively low N₂ fixation rates. These results indicate that Ni deficiency limits the growth of the *Cyanothece* to some extent, considerably decreases H₂ uptake by hydrogenase and leads to H₂ accumulation and N₂ fixation variation in the diazotroph. The findings show that Ni availability is a critical factor on controlling H₂ production and N₂ fixation in marine diazotrophic cyanobacteria. The information of Ni bioavailability for diazotrophic cyanobacteria is thus essential to evaluate the importance of Ni for H₂ cycling and N₂ fixation in oceanic surface waters.

Marine nitrogen-fixing cyanobacteria play important roles in regulating nitrogen and carbon cycling globally by transforming dinitrogen (N₂) to bioavailable nitrogen, ammonia (NH₃) (Karl et al. 2002; Bonnet et al. 2011). In addition to producing ammonia, hydrogen gas (H₂) is generated simultaneously as a byproduct through nitrogen fixation process as shown in Eq. 1:



It has been widely observed that H₂ concentrations are supersaturated in the surface water of the tropical and subtropical oceans and the concentrations are closely related to cyanobacterial N₂ fixation activities. Early field studies observed that *Trichodesmium*, one of the major oceanic diazotrophic cyanobacteria, produces substantial amount of H₂ in the Caribbean Sea and the Atlantic Ocean (Scranton 1983, 1984; Scranton et al. 1987). In the North Pacific, Moore et al. (2009) also showed that net N₂ fixation rates exhibited a strong positive correlation with H₂ concentrations ($r = 0.96$), which ranged from 0.30 to 12.6 nmol L⁻¹ and were higher than its corresponding seawater equilibrium concentrations under H₂ atmospheric partial pressure. In the Atlantic Ocean, it was reported that H₂ concentrations were positively correlated with the

abundances of *Candidatus Atelocyanobacterium thalassa* ($r = 0.77$), a dominant unicellular diazotrophic cyanobacterium (Moore et al. 2018). Laboratory culture studies also showed that prevalent marine diazotrophic cyanobacteria, including *Trichodesmium*, *Crocospaera*, and *Cyanothece*, produced significant amount of H₂ during N₂ fixation process (Punshon and Moore 2008; Wilson et al. 2010a,b, 2012). In brief, both field and laboratory studies have demonstrated that cyanobacterial N₂ fixation is the major source of supersaturated H₂ in the upper ocean.

In terms of the stoichiometry in the nitrogen fixation reaction, the molar ratio of N₂ fixed to H₂ produced is 1:1 (Eq. 1). However, all of the measured ratios of net H₂ produced to N₂ fixed (hereafter the H₂:N₂ ratios) were less than 1 and varied significantly in both the field and laboratory studies. Field studies in the Caribbean Sea and the Atlantic Ocean (Scranton 1983, 1984; Scranton et al. 1987) reported that the H₂:N₂ ratio in *Trichodesmium* varied from 0.008 to 0.64. Laboratory studies showed that the H₂:N₂ ratios varied extensively for all of major diazotrophic cyanobacteria among different studies, such as 0.003–0.016 for *Crocospaera*, 0.040–0.055 for *Cyanothece*, and 0.15–0.48 for *Trichodesmium* (Punshon and Moore 2008; Wilson et al. 2010a,b, 2012). The effort to apply H₂ production rates to estimate N₂ fixation rates, or vice versa, was hindered by the huge variations (Wilson et al. 2013; Moore et al. 2014). It has still remained unclear what environmental factors regulate the enormous variations and H₂ accumulation.

Since uptake hydrogenase oxidizes H₂ to proton and electron concurrently during N₂ fixation (Tamagnini et al. 2007), the oxidation would result in the decline of H₂ produced and

*Correspondence: tyho@gate.sinica.edu.tw

Additional Supporting Information may be found in the online version of this article.

^aPresent address: Marine Science Institute, University of the Philippines Diliman, Quezon, Philippines

the molar ratio of H₂ produced to N₂ fixed to be less than 1. Indeed, hydrogen oxidation by uptake hydrogenase is beneficial to N₂ fixation since H₂ can inhibit nitrogenase activity (Guth and Burris 1983; Tamagnini et al. 2007). Moreover, uptake hydrogenase in unicellular diazotrophic cyanobacteria may also play a role on protecting nitrogenase from oxygen (O₂) toxicity (Zhang et al. 2014). In addition to uptake hydrogenase, diazotrophic cyanobacteria may contain a bidirectional hydrogenase, an enzyme generally existing in the nondiazotrophic cyanobacteria and being capable of regulating H₂ production and recycling with NAD(P)⁺ and NAD(P)H reversibly (Tamagnini et al. 2007). However, the role of bidirectional hydrogenase on H₂ removal in diazotrophic cyanobacteria is not significant as uptake hydrogenase (Masukawa et al. 2002; Zhang et al. 2014). As cyanobacterial uptake hydrogenases are NiFe-bearing enzymes, Ni is expected to be a crucial factor for H₂ uptake in diazotrophic cyanobacteria. Indeed, previous freshwater culture studies showed that high Ni addition from 10 to 17,000 nmol L⁻¹ inhibited H₂ production for diazotrophic cyanobacteria *Anabaena cylindrica* and *Oscillatoria subbrevis* (Daday and Smith 1983; Xiankong et al. 1984; Daday et al. 1985; Kumar and Polasa 1991). However, total dissolved Ni concentrations are generally around 2 nmol L⁻¹ in the surface waters of the tropical and subtropical open oceans (Bruland et al. 1979; Mackey et al. 2002; Wang et al. 2014; Schlitzer et al. 2018) so that the abnormally high Ni concentrations and nontrace metal buffered condition used in the freshwater study cannot reflect the impact of Ni deficiency on marine diazotrophic cyanobacteria. Although the Ni concentrations are around 2 nmol L⁻¹, the concentration level is one of the highest in comparison with other biologically essential trace metals in the surface water, such as Fe, Co, and Zn. It remains unclear whether 2 nmol L⁻¹ dissolved Ni level may limit the growth of some phytoplankton with Ni enzymes (Dupont et al. 2010; Ho 2013). Our previous laboratory culture experiments have demonstrated that Ni availability influences the growth and N₂ fixation of *Trichodesmium* (Ho 2013; Ho et al. 2013; Rodriguez and Ho 2014), which also show that a trace metal-defined culture medium with a low Ni background (Ho 2013) is essential to investigate the impact of Ni deficiency on marine phytoplankton.

Among major marine unicellular diazotrophic cyanobacteria (Luo et al. 2012; Cheung et al. 2017), *Cyanothece* strain ATCC 51142, hereafter *Cyanothece*, has been widely used as a model diazotrophic cyanobacterium for H₂ production studies (Bandyopadhyay et al. 2010, 2011; Min and Sherman 2010; Wilson et al. 2010a; Aryal et al. 2013). Its decoded genome also indicates that it possesses NiFe-uptake hydrogenases (Welsh et al. 2008; Bandyopadhyay et al. 2010). Most importantly, *Cyanothece* does not possess urease and Ni-superoxide dismutase (NiSOD) (Welsh et al. 2008) so that the effect of Ni deficiency is most likely manifest through effects on uptake hydrogenase. The major objective of this study is to investigate the effects of Ni deficiency on H₂ accumulation

and N₂ fixation in *Cyanothece* and the implication on understanding the environmental control on H₂ cycling and N₂ fixation rates in the ocean.

Methods

Cyanothece sp. ATCC 51142 was obtained from American Type Culture Collection. Batch cultures of the strain were grown in 1-liter trace metal-clean polycarbonate Erlenmeyer flasks with 500 mL of trace metal-defined medium (Supporting Information Table S1) modified from YBCII recipe (Chen et al. 1996; Ho 2013). To prepare the trace metal-defined YBCII medium, we removed trace metal impurities from the artificial seawater base and working stocks of phosphate by passing the solutions through quartz column filling with chelating resins (Chelex[®] 100, Bio-Rad) in a clean room (Ho 2013). Sterilization and preparation for the medium followed the procedures for preparing trace metal-defined culture media (Price et al. 1989; Ho et al. 2003). All cultures were kept in an incubator with orbital shaking speed at 45 revolutions min⁻¹, temperature controlled at 26°C, and illumination at photon flux density of 450 μmol quanta m⁻² s⁻¹ operated at a 12:12 h light:dark square wave cycle.

To examine the effects of Ni under different Fe supplies, we conducted a 3 × 2 factorial design for the experiments. Three levels of total dissolved Ni supply, 0.03 nmol L⁻¹ (background concentration of the culture medium without Ni addition, low Ni treatment), 10 nmol L⁻¹ (medium Ni treatment), and 100 nmol L⁻¹ (high Ni treatment) were set under two levels of Fe addition, with total dissolved Fe concentrations to be 100 and 400 nmol L⁻¹. Trace metal availability was buffered by adding 20 μmol L⁻¹ ethylenediaminetetraacetic acid (EDTA). Each Ni-Fe treated culture was acclimated for around 20 generations (about 2 months) before performing the formal experiments (Supporting Information Table S2). Each treatment of batch culture had three replicate polycarbonate flasks for the formal experiments. In addition to the formal experiments, the samples obtained from the preliminary experiments during the acclimation process were also measured (Supporting Information Table S2).

We monitored cell density (cells mL⁻¹) and cell volume (μm³ cell⁻¹) almost every day using a Multisizer 3 particle counter (Beckman Coulter). Specific growth rate (d⁻¹) was calculated using cell density data acquired during the late exponential growth phase, generally ranging from 10⁵ to 2 × 10⁶ cells mL⁻¹ (Fig. 1). Culture samples were concurrently processed during the late exponential phase for the measurement of the following parameters, including H₂ accumulation and N₂ fixation rates, elemental quotas, and chlorophyll *a* (hereafter Chl *a*) content. The sampling time for each treatment was labeled with asterisk at the lower right position of the data point (Fig. 1). It should be noticed that the cells grown in the treatments with medium Ni-high Fe (all the replicates) and high Ni-low Fe (one of the replicates) concentrations had entered the

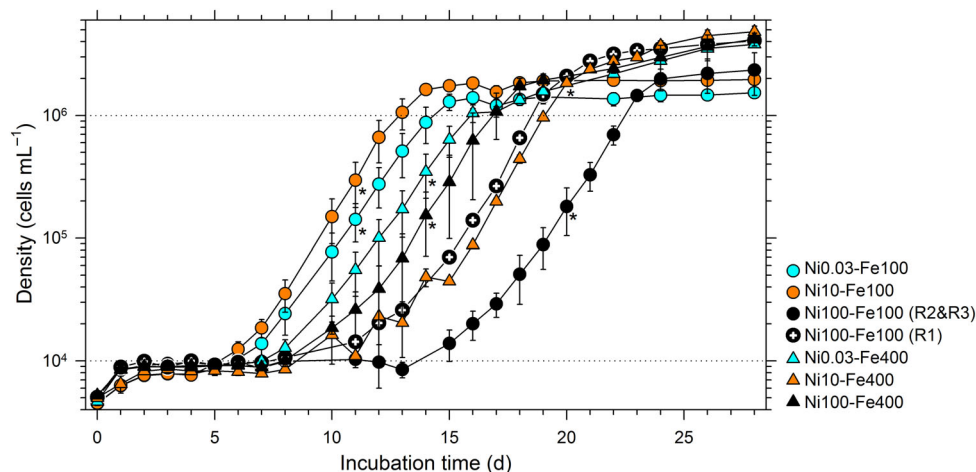


Fig. 1. Growth curves of *Cyanothece* under various Ni and Fe treatments. The number next to elemental symbol (Ni) stands for total dissolved Ni concentration, which was either 0.03, 10, or 100 nmol L⁻¹. The Fe concentrations were either 100 or 400 nmol L⁻¹. Error bars stand for 1 SD from the average. For Ni100-Fe100 treatment, one replicate (R1) is not combined with the other two (R2 and R3) due to their unsynchronized growth paces. Asterisk below a symbol indicates the time point for the measurements of cell volume, Chl *a* contents, cellular elemental quotas, and rates of H₂ accumulation and N₂ fixation.

early stationary phase when collecting samples for the measurements (Fig. 1).

We measured the rates of H₂ accumulation and N₂ fixation by mercury oxide (HgO) reduction technique (Herr et al. 1981) and acetylene (C₂H₂) reduction (Capone and Montoya 2001), respectively. Two hours before the dark period started, each 10 mL aliquot of culture grown from each replicate flask under each treatment was transferred to a 20 mL vial and was crimp-sealed using Teflon-coated cap in a clean room. For H₂ measurements, the vials were incubated in the dark for 12 h. After incubation, H₂ concentrations were measured by injecting the gaseous samples into a 0.1 mL sample loop of a Peak Performer 1 Reducing Compound Photometer (Peak Laboratories) equipped with a heated HgO bed and UV absorption detector. For N₂ fixation assay, 2 mL of the headspace gas in the vials was sucked out and replaced with 2 mL of commercially available C₂H₂ by needles, then the vials were incubated in the dark for 12 h. After incubation, 1 mL of the headspace gas from each vial was drawn for the measurement every 2 h during the incubation period. N₂ fixation was estimated by analyzing ethylene (C₂H₄) production using an Agilent 7890A gas chromatograph with a Poropak N column (Agilent, HP-PLOT Al₂O₃ S) and a flame ionization detector. The N₂ fixation rate was calculated using a reduction ratio (C₂H₂:N₂) of 4:1 for the conversion (Capone and Montoya 2001; Punshon and Moore 2008; Wilson et al. 2010a). Both the rates were normalized to cell volume subjected to the respective assays. We have used the data point of 12-h yield in the dark to calculate the daily rate (amol μm⁻³ d⁻¹). The time-series hourly rates (amol μm⁻³ h⁻¹) were also calculated by subtracting accumulated H₂/C₂H₄ concentrations observed at the preceding point then divided by the duration.

The elemental quotas were determined by collecting cells with 2 μm acid-washed polycarbonate membrane filters for P and trace metal analysis and precombusted GF/F filters for C and N analysis at the middle of the dark period. For phosphorus and trace metal analysis, the harvested cells were washed with ultrapure water to remove the culture medium residue in a class 100 trace metal clean laboratory. The filters with cells were digested using super pure concentrated nitric acid (ULTREX II, JT-Baker) in trace metal clean Teflon vials prior to elemental analyses using high-resolution inductively coupled plasma mass spectrometer (Element XR, Thermo Scientific). For C and N analysis, the harvested cells were fumed for 24 h with concentrated hydrochloric acid to remove particulate inorganic carbon prior to measurement by an elemental analyzer (2400 CHNS/O Series II, PerkinElmer). Filter blanks were subjected to the same digestion, dilution, and analysis. The blank values were subtracted from sample measurements. The details of the analytical precision, accuracy, and detection limits of the pretreatment and inductively coupled plasma mass spectrometry method for elemental measurement were described in our previous studies (Ho et al. 2003; Ho 2013).

Cells for Chl *a* concentration measurements were harvested by filtration onto GF/F filters at the middle of the dark period. The filters were preserved in tissue embedding cassettes and were kept frozen at -80°C until further processing. Water content from the filters was removed by freeze-drying the filters for 24 h prior to Chl *a* extraction in dark by using 90% acetone with sonication in an ice slurry for 1 h. Extracted Chl *a* samples were then filtered through a 0.2-μm filter to remove particulate debris and subsequently analyzed by high-performance liquid chromatography (LC-10A, Shimadzu). The Chl *a* concentrations measured include both mono-Chl *a* and

divinyl-Chl *a*. The details of the method were described in our previous study (Ho et al. 2015).

Data acquired at the early stationary phase, including one replicate of the treatment with high Ni-low Fe as well as all three replicates of the treatment with medium Ni-high Fe (the treatment as a missing cell) (Supporting Information Tables S3–S6), were not included into the statistical data sets for comparisons among different Ni and Fe treatments. Responses among different Ni and Fe treatments were compared using two-way ANOVA and post hoc Tukey's studentized range test (only for the balanced data of specific growth rate) or Tukey–Kramer test. For such unbalanced data sets with the missing cell, a Type IV sum-of-square method was applied for ANOVA. If the interaction effect between Ni and Fe was significant ($p < 0.05$), then the post hoc test would be performed to investigate the difference among the Ni-Fe treatments. Relationships between the rates of H₂ accumulation and N₂ fixation as well as between the H₂:N₂ ratio and total dissolved Ni concentrations were tested with Pearson's correlation coefficient (r). The data used for correlation test were log₁₀-transformed. Student's *t*-tests were applied to compare the differences on elemental quotas between cells harvested at the early stationary and late exponential phases. All the data were presented as mean \pm 1 standard deviation (SD). All statistical procedures were carried out by SAS program (SAS Institute).

Results

Cyanothece showed relatively low growth rates in the treatments without Ni addition, in which the growth rate (0.63 d⁻¹) was corresponding to 84% of maximal growth rates (0.75 d⁻¹) obtained from the medium Ni-high Fe treatment (Fig. 2a; Supporting Information Tables S3, S7). In the low Ni treatments, cell volume was larger than the medium and high Ni treatments (Fig. 2b; Supporting Information Tables S3, S7). We found that the effects of low Ni treatments on growth rates and cellular volume were repeatedly observed in the low Ni treatments in both formal experiments (Fig. 2a,b) and preliminary experiments (Supporting Information Fig. S1). No significant difference on Chl *a* content was found among the treatments (Fig. 2c; Supporting Information Tables S3, S7).

Cellular elemental compositions are shown in Figs. 3, 4. Due to the significant variations of cell volume among different Ni treatments, elemental quota and rate parameters were presented by being normalized to cell volume. Except the treatment harvested at the early stationary phase, the averaged quotas of C, N, and P for all other treatments ranged from 8.4 to 13, from 2.4 to 2.7, and from 0.036 to 0.048, respectively (Fig. 3a–c; Supporting Information Tables S4, S7). No significant differences on the quotas of N and P were found (Fig. 3b,c; Supporting Information Tables S4, S7). In terms of trace metal quota, cellular Ni quota positively responded to Ni availability, possessing quotas ranging from 0.6 to 1.4 zmol μm^{-3} for the low Ni treatments and from 29 to 34 zmol μm^{-3} for the high

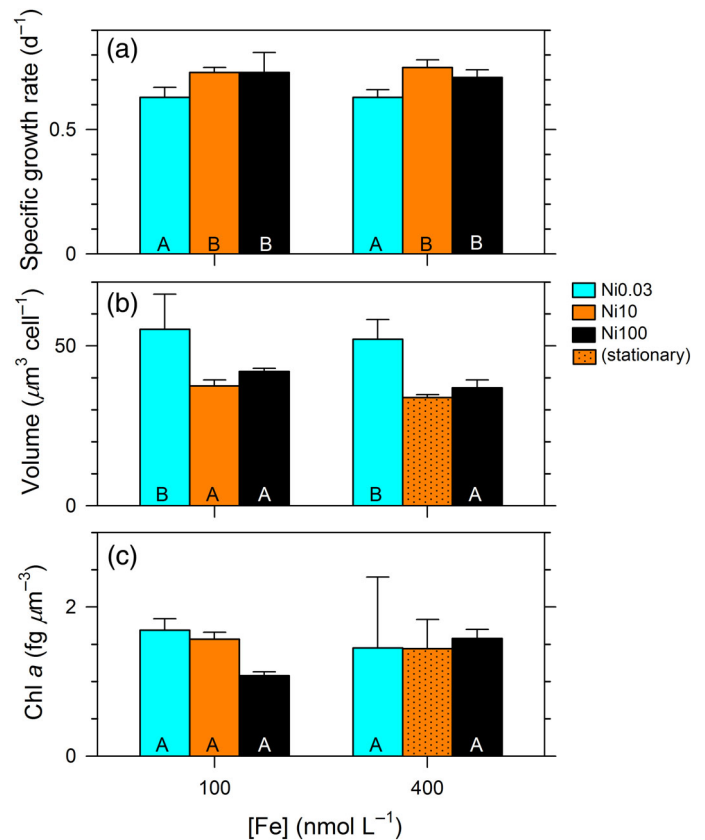


Fig. 2. Specific growth rates (a), cell volume (b), and Chl *a* concentrations (c) in *Cyanothece* at the late exponential growth phase under various Ni and Fe treatments. The total dissolved Ni supply were 0.03, 10, and 100 nmol L⁻¹. Error bars stand for 1 SDs from the average. Data acquired at the early stationary phase were excluded from statistical tests (Supporting Information Tables S3, S7). By two-way ANOVA, the Ni \times Fe interaction effect and Fe main effect were not significant ($p > 0.05$) on the growth rate, volume, and Chl *a* concentration (Supporting Information Table S7). Different letters denote a significant difference ($p < 0.05$) among different Ni treatments.

Ni treatments of both high and low Fe treatments (Fig. 4a; Supporting Information Tables S5, S7). No significant difference was observed for other trace metal quotas, Co, Mo, Cd, Cu, and Mn (Fig. 4c,d,f–h).

The H₂ accumulation rates increased and N₂ fixation rates decreased overall with decreasing Ni supply (Fig. 5). In the low Ni treatments, averaged H₂ accumulation rates, ranging from 20.8 to 26.8 amol H₂ μm^{-3} d⁻¹, were fivefold to twentyfold higher than those obtained in the higher Ni treatments, ranging from 1.1 to 4.0 amol H₂ μm^{-3} d⁻¹ (Fig. 5a; Supporting Information Table S6). These trends on H₂ accumulation and N₂ fixation were also repeatedly observed in the preliminary experiments (Supporting Information Fig. S2). Although the correlation between the rates of H₂ accumulation and N₂ fixation was not significant for the formal experiment alone ($r = -0.30$, $n = 14$, $p = 0.29$), combining the data of preliminary and formal experiments all

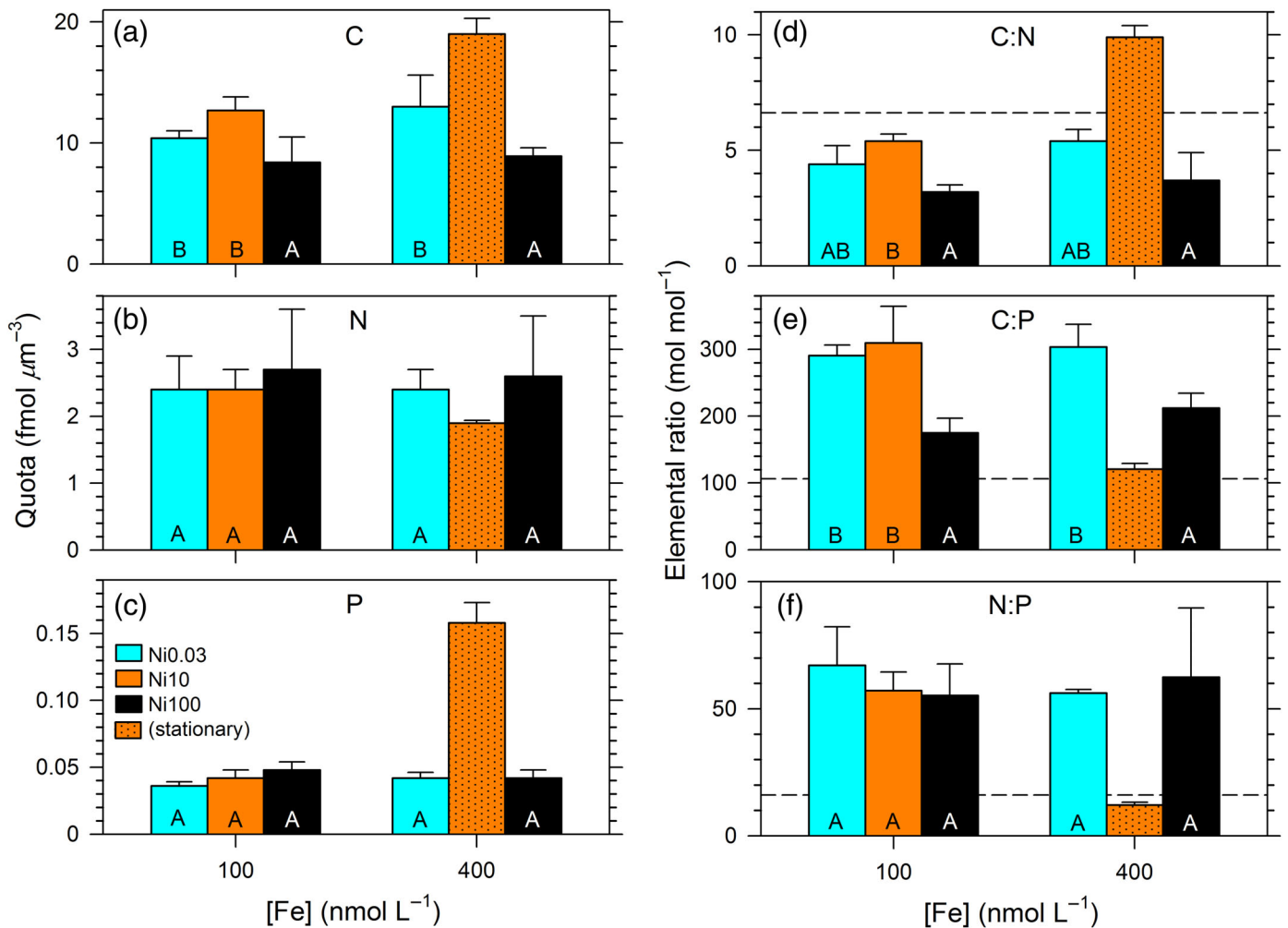


Fig. 3. Cell volume-normalized major elemental quotas (a–c) and ratios (d–f) in *Cyanothece* at the late exponential growth phase under various Ni and Fe treatments. The total dissolved Ni supply were 0.03, 10, and 100 nmol L^{-1} . Error bars stand for 1 SDs from the average. Dashed lines stand in (d–f) stand for the Redfield ratio. Data acquired at the early stationary phase were excluded from statistical tests (Supporting Information Tables S4, S7). By two-way ANOVA, the Ni \times Fe interaction effect and Fe main effect were not significant ($p > 0.05$) on the quotas and ratios (Supporting Information Table S7). Different letters denote a significant difference ($p < 0.05$) among different Ni treatments.

together, the H_2 accumulation rate was negatively correlated with N_2 fixation rate ($r = -0.48$, $n = 24$, $p < 0.05$) (Fig. 6).

Discussion

The results of Fig. 2a demonstrate that Ni deficiency can limit the growth of *Cyanothece* to some extent, with growth rates decreasing 13–24% from the maximal observed growth rates. The condition of Ni deficiency was validated by the corresponding decreasing Ni quotas among the treatments (Fig. 4a). In addition to the impact on growth rate, our study revealed that Ni limitation in *Cyanothece* causes significant H_2 accumulation, with one order of magnitude higher accumulation rates in the low Ni treatments than medium and high Ni treatments (Fig. 5a). The results suggest that the production of NiFe-uptake hydrogenases was hindered owing to Ni deficiency.

The results of Figs. 5, 6 and Supporting Information Fig. S2 clearly show that Ni availability regulates H_2 accumulation and N_2 fixation in *Cyanothece*. As H_2 is a competitive inhibitor for nitrogenase (Guth and Burris 1983; Tamagnini et al. 2007), elevated H_2 accumulation caused by deficient Ni supply would concurrently hinder N_2 fixation. Under the condition of sufficient Ni supply, the ample production of NiFe-uptake hydrogenase would reduce H_2 level (Daday and Smith 1983; Xiankong et al. 1984; Daday et al. 1985; Kumar and Polasa 1991) and maintain N_2 fixation activities. The pooled daily based data showed a significant negative relationship between the rates of H_2 accumulation and N_2 fixation (Fig. 6). Similarly, we also observed that the variations of N_2 fixation rates and H_2 accumulation rates seem to be inverse during the dark period (Supporting Information Figs. S3, S4). Both the daily and hourly rates suggest that H_2 removal by uptake hydrogenase enhances nitrogenase activities

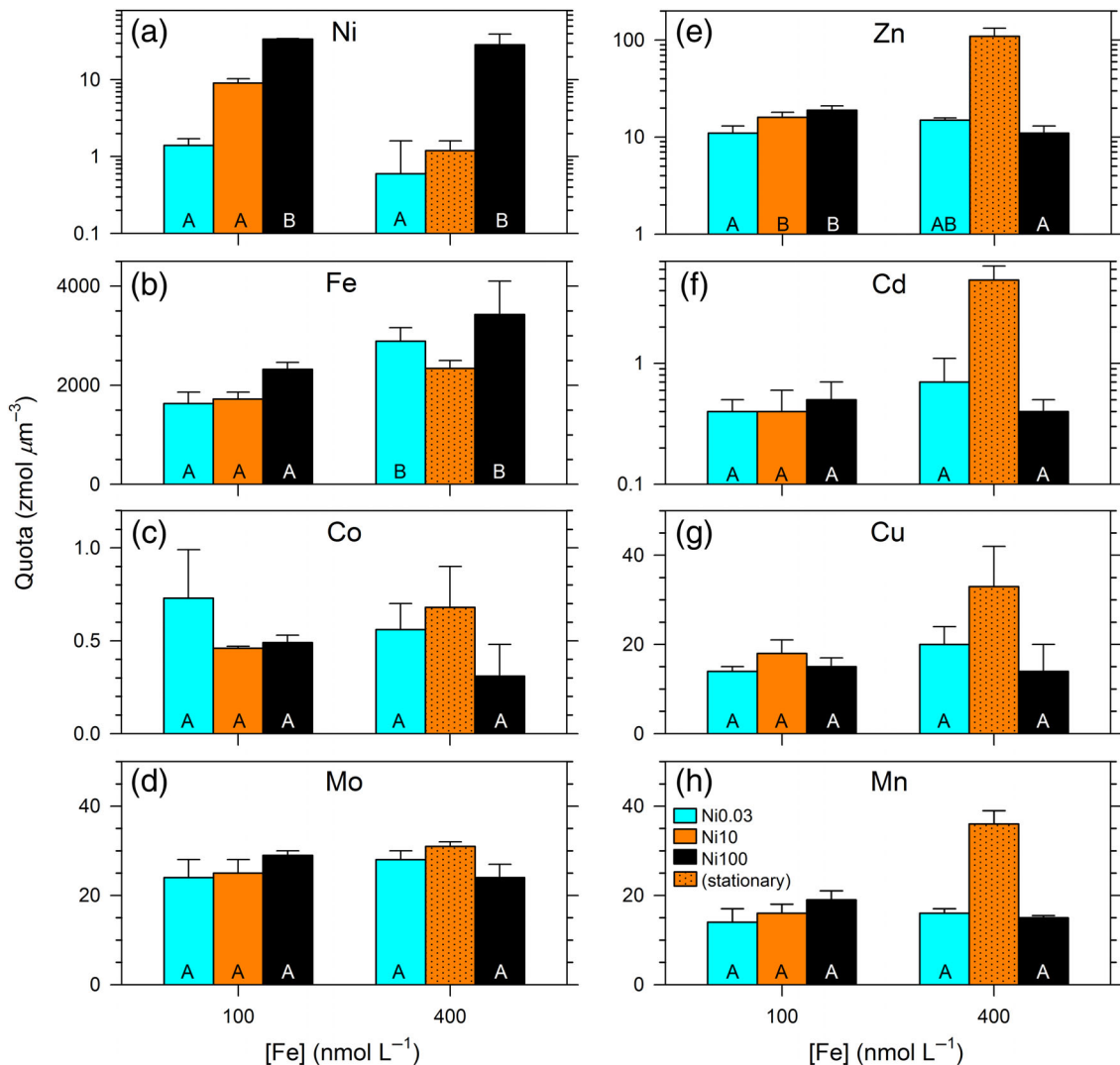


Fig. 4. Cell volume-normalized trace metal quotas in *Cyanothece* at the late exponential growth phase under various Ni and Fe treatments. The total dissolved Ni supply were 0.03, 10, and 100 nmol L^{-1} . Error bars stand for 1 SDs from the average. Data acquired at the early stationary phase were excluded from statistical tests (Supporting Information Tables S5, S7). By two-way ANOVA, the Ni \times Fe interaction effect was not significant ($p > 0.05$) on Ni, Fe, Co, Cd, and Cu quotas; among these quotas, the Fe main effect was significant ($p < 0.05$) only on Fe quota. On the other hand, the Ni \times Fe interaction effect was significant ($p < 0.05$) on Mo, Zn, and Mn quotas. The post hoc tests were performed to investigate the difference on Mo, Zn, and Mn quotas among the Ni-Fe treatments (Supporting Information Table S7). Different letters denote a significant difference ($p < 0.05$) among different Ni treatments (a, c, f, g), between Fe treatments (b), or among Ni-Fe treatments (d, e, h).

and results in elevated N_2 fixation rates overall. Indeed, previous study clearly demonstrated that nitrogenase expression was hindered in *Cyanothece* mutant with an uptake hydrogenase subunit knockout (Zhang et al. 2014), showing the essential role of uptake hydrogenase on cyanobacterial N_2 fixation. For the treatments with 400 nmol L^{-1} Fe supply, N_2 fixation rates were all relatively low for all three Ni groups (Fig. 5b). It is unclear to us why the N_2 fixation rates were relatively low for the high Ni-high Fe treatment. In addition, it should be noticed that the daily N_2 fixation rates estimated from 12-h short-term integration may not be representative to calculate the overall biomass N due to various uncertainties involved (Supporting Information

Text S1). In brief, under Ni deficiency condition, our experiments suggest that increasing H_2 accumulation rates would cause the decline of N_2 fixation rates.

Figure 7 shows that bioavailable Ni concentration is an important factor controlling the variations of the $H_2:N_2$ ratios in *Cyanothece*. The highly varied ratios were negatively correlated with Ni concentrations ($r = -0.71$, $n = 14$, $p < 0.01$). A previous laboratory study showed significant differences on the ratio among various diazotrophic cyanobacteria and the authors argued that the two orders of magnitude differences reflected the ability of H_2 reutilization among the species (Wilson et al. 2010a). Supposedly, while expressing urease or

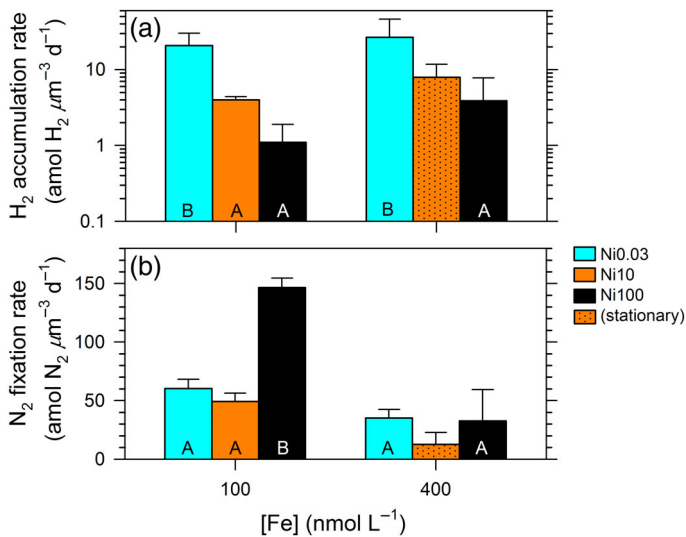


Fig. 5. Cell volume-normalized rates of H₂ accumulation (a) and N₂ fixation (b) in *Cyanothecce* at the late exponential growth phase under various Ni and Fe treatments. The total dissolved Ni supply were 0.03, 10, and 100 nmol L⁻¹. Error bars stand for 1 SDs from the average. Data acquired at the early stationary phase were excluded from statistical tests (Supporting Information Tables S6, S7). By two-way ANOVA, the Ni × Fe interaction effect and Fe main effect were not significant ($p > 0.05$) on H₂ accumulation rate. On the other hand, the Ni × Fe interaction effect was significant ($p < 0.05$) on N₂ fixation rate. The post hoc test was performed to investigate the difference on N₂ fixation rate among the Ni-Fe treatments (Supporting Information Table S7). Different letters denote a significant difference ($p < 0.05$) among Ni treatments (a) or among Ni-Fe treatments (b).

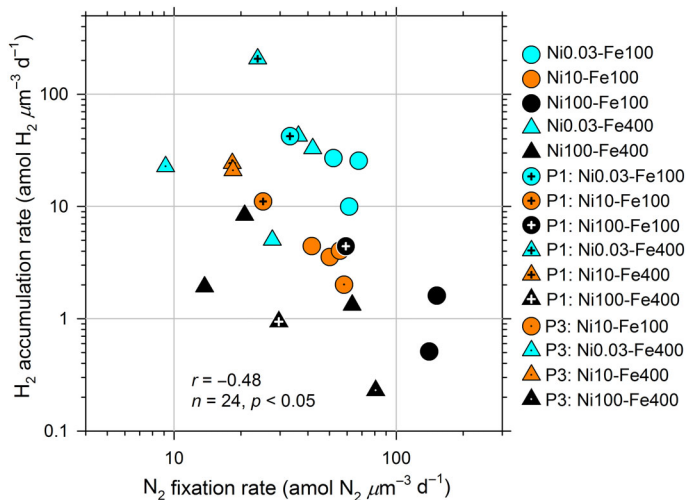


Fig. 6. Comparison between cell volume-normalized H₂ accumulation and N₂ fixation rates in *Cyanothecce* at the late exponential growth phase under various Ni and Fe treatments. Data include the experiments carried out in the formal (Fig. 5) and preliminary (P1 and P3, Supporting Information Fig. S2) experiments. Data for P2 experiments were not included as the cells were all harvested at the early stationary phase. The number next to elemental symbol (Ni) stands for total dissolved Ni concentration, which was either 0.03, 10, or 100 nmol L⁻¹. Same to Fe, either 100 or 400 nmol L⁻¹.

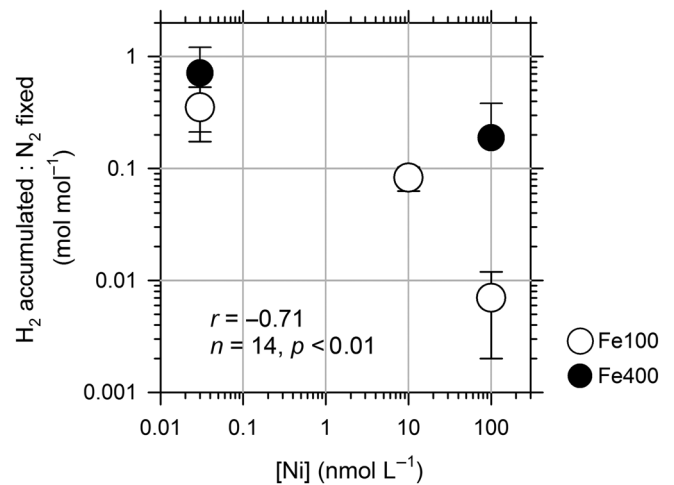


Fig. 7. Comparison between Ni supply and the H₂:N₂ ratio in *Cyanothecce* at the late exponential growth phase under various Ni and Fe treatments.

NiSOD (Ho 2013), these two diazotrophs are expected to require more Ni than *Cyanothecce* and exhibit higher H₂:N₂ ratios than *Cyanothecce* if they all grow under the same level of low Ni supply. It should be noticed that the culture media used in the study (Wilson et al. 2010a), either natural seawater-based SO (Waterbury and Willey 1988) or artificial seawater-based YBCII (Chen et al. 1996), were not added with Ni and were not trace metal defined so that the conditions of bioavailable Ni concentrations were possibly inconsistent in the experiments. It is thus essential to use a trace metal-defined culture medium to study N₂ fixation rates or the H₂:N₂ ratios of diazotrophic cyanobacteria by laboratory culture experiments. The results of Fig. 7 imply that the H₂:N₂ ratios of some diazotrophic cyanobacterial species may also vary significantly in the field with different Ni availability in ambient seawater. The condition of Ni availability can be a potential cause for the huge variations of the H₂:N₂ ratios (0.008–0.64) observed in *Trichodesmium* colonies collected in the surface seawaters of the Caribbean Sea and the Atlantic Ocean (Scranton 1983, 1984; Scranton et al. 1987).

The results of Fig. 5a suggest that Ni availability can be an important factor causing the huge variations of H₂ concentrations observed in oceanic surface water. Although both H₂ concentrations and N₂ fixation rates varied considerably in the tropical and subtropical oceans (Moore et al. 2009, 2018; Chen et al. 2014), field data show that total dissolved Ni concentrations are relatively comparable in the surface water (Bruland et al. 1979; Mackey et al. 2002; Wang et al. 2014; Schlitzer et al. 2018), around 2 nmol L⁻¹. Unlike Fe and Cu which are strongly chelated by organic ligands in the surface water, studies showed that a significant portion (40–80%) of dissolved Ni in the surface water is labile (Achterberg and van den Berg 1997; Saito et al. 2004; Boiteau et al. 2016), which was operationally determined by the exchangeable dissolved

Ni with 12-h 20- $\mu\text{mol L}^{-1}$ dimethylglyoxime treatment. It remains unclear whether this relatively weakly bound labile Ni are bioavailable to diazotrophic cyanobacteria or not (Ho 2013). Although the study of Boiteau et al. (2016) provided preliminary information about the elemental composition of Ni organic ligand extracted, the extracted fraction only accounted for 1–2% of total Ni concentrations. Further studies should focus on developing methods to investigate the structure and bioavailability of the majority of total dissolved Ni in the surface water. Then we may be able to assess whether Ni supply can serve as a critical variable for the H₂ cycling and N₂ fixation of diazotrophic cyanobacteria in the ocean.

In addition to Ni availability in seawater, biological Ni demand may vary significantly among different diazotrophic cyanobacterial groups, attributed to the difference of their intracellular Ni-containing enzymes. As mentioned previously, both *Trichodesmium* and *Crocospaera* contain NiFe hydrogenase, NiSOD, and urease (Dupont et al. 2008). It deserves further study to investigate their Ni requirement, the expressions of Ni-containing enzymes, and the impacts on N₂ fixation and H₂ production under various Ni supply in different oceanic regions. Enzymatic antibody approach and in situ Ni enrichment experiments may be applied to validate the importance of individual enzyme among different diazotrophic cyanobacteria. How Ni supply controls the dynamics of H₂ concentration and N₂ fixation in the ocean deserves further investigation.

Conclusion

Ni limitation in *Cyanothece* resulted to elevated H₂ accumulation and caused the variations on N₂ fixation rates. These results indicate that Ni deficiency decreases H₂ uptake and occasionally N₂ fixation, leading to a decline in growth rate while cellular N quota keeps constant. Our findings suggest that H₂ supersaturation in the upper ocean may thus be associated with Ni bioavailability for diazotrophic cyanobacteria. Ni bioavailability in oceanic surface water would be essential information to evaluate the role of Ni on H₂ cycling and N₂ fixation for marine diazotrophic cyanobacteria. Moreover, in situ Ni enrichment experiments can be carried out to demonstrate the importance of Ni on cyanobacterial H₂ cycling and N₂ fixation in the ocean, which can be elucidated via examining the expressions of uptake hydrogenase and nitrogenase.

References

- Achterberg, E. P., and C. M. G. van den Berg. 1997. Chemical speciation of chromium and nickel in the western Mediterranean. *Deep-Sea Res. Part II Top. Stud. Oceanogr.* **44**: 693–720. doi:10.1016/S0967-0645(96)00086-0
- Aryal, U. K., and others. 2013. Proteome analyses of strains ATCC 51142 and PCC 7822 of the diazotrophic cyanobacterium *Cyanothece* sp. under culture conditions resulting in enhanced H₂ production. *Appl. Environ. Microbiol.* **79**: 1070–1077. doi:10.1128/AEM.02864-12
- Bandyopadhyay, A., J. Stöckel, H. Min, L. A. Sherman, and H. B. Pakrasi. 2010. High rates of photobiological H₂ production by a cyanobacterium under aerobic conditions. *Nat. Commun.* **1**: 139. doi:10.1038/ncomms1139
- Bandyopadhyay, A., T. Elvitigala, E. Welsh, J. Stöckel, M. Liberton, H. Min, L. A. Sherman, and H. B. Pakrasi. 2011. Novel metabolic attributes of the genus *Cyanothece*, comprising a group of unicellular nitrogen-fixing Cyanobacteria. *mBio* **2**: e00214–11. doi:10.1128/mBio.00214-11
- Boiteau, R. M., and others. 2016. Structural characterization of natural nickel and copper binding ligands along the US GEOTRACES Eastern Pacific Zonal Transect. *Front. Mar. Sci.* **3**: 243. doi:10.3389/fmars.2016.00243
- Bonnet, S., O. Grosso, and T. Moutin. 2011. Planktonic dinitrogen fixation along a longitudinal gradient across the Mediterranean Sea during the stratified period (BOUM cruise). *Biogeosciences* **8**: 2257–2267. doi:10.5194/bg-8-2257-2011
- Bruland, K. W., R. P. Franks, G. A. Knauer, and J. H. Martin. 1979. Sampling and analytical methods for the determination of copper, cadmium, zinc, and nickel at the nanogram per liter level in sea water. *Anal. Chim. Acta* **105**: 233–245. doi:10.1016/S0003-2670(01)83754-5
- Capone, D. G., and J. P. Montoya. 2001. Nitrogen fixation and denitrification. *Methods Microbiol.* **30**: 501–515. doi:10.1016/S0580-9517(01)30060-0
- Chen, Y.-B., J. P. Zehr, and M. Mellon. 1996. Growth and nitrogen fixation of the diazotrophic filamentous nonheterocystous cyanobacterium *Trichodesmium* sp. IMS 101 in defined media: Evidence for a circadian rhythm. *J. Phycol.* **32**: 916–923. doi:10.1111/j.0022-3646.1996.00916.x
- Chen, Y. L. L., H. Y. Chen, Y. H. Lin, T. C. Yong, Y. Taniuchi, and S. Tuo. 2014. The relative contributions of unicellular and filamentous diazotrophs to N₂ fixation in the South China Sea and the upstream Kuroshio. *Deep-Sea Res. Part I Oceanogr. Res. Pap.* **85**: 56–71. doi:10.1016/j.dsr.2013.11.006
- Cheung, S., K. Suzuki, H. Saito, Y. Umezawa, X. Xia, and H. Liu. 2017. Highly heterogeneous diazotroph communities in the Kuroshio Current and the Tokara Strait, Japan. *PLoS One* **12**: e0186875. doi:10.1371/journal.pone.0186875
- Daday, A., and G. D. Smith. 1983. The effect of nickel on the hydrogen metabolism of the cyanobacterium *Anabaena cylindrica*. *FEMS Microbiol. Lett.* **20**: 327–330. doi:10.1111/j.1574-6968.1983.tb00141.x
- Daday, A., A. H. Mackerras, and G. D. Smith. 1985. The effect of nickel on hydrogen metabolism and nitrogen fixation in the cyanobacterium *Anabaena cylindrica*. *Microbiology* **131**: 231–238. doi:10.1099/00221287-131-2-231
- Dupont, C. L., K. Barbeau, and B. Palenik. 2008. Ni uptake and limitation in marine *Synechococcus* strains. *Appl. Environ. Microbiol.* **74**: 23–31. doi:10.1128/AEM.01007-07

- Dupont, C. L., K. N. Buck, B. Palenik, and K. Barbeau. 2010. Nickel utilization in phytoplankton assemblages from contrasting oceanic regimes. *Deep-Sea Res. Part I Oceanogr. Res. Pap.* **57**: 553–566. doi:10.1016/j.dsr.2009.12.014
- Guth, J. H., and R. H. Burris. 1983. Inhibition of nitrogenase-catalyzed NH_3 formation by H_2 . *Biochemistry* **22**: 5111–5122. doi:10.1021/bi00291a010
- Herr, F. L., M. I. Scranton, and W. R. Barger. 1981. Dissolved hydrogen in the Norwegian Sea: Mesoscale surface variability and deep-water distribution. *Deep-Sea Res. Part A Oceanogr. Res. Pap.* **28**: 1001–1016. doi:10.1016/0198-0149(81)90014-5
- Ho, T.-Y. 2013. Nickel limitation of nitrogen fixation in *Trichodesmium*. *Limnol. Oceanogr.* **58**: 112–120. doi:10.4319/lo.2013.58.1.0112
- Ho, T.-Y., A. Quigg, Z. V. Finkel, A. J. Milligan, K. Wyman, P. G. Falkowski, and F. M. M. Morel. 2003. The elemental composition of some marine phytoplankton. *J. Phycol.* **39**: 1145–1159. doi:10.1111/j.0022-3646.2003.03-090.x
- Ho, T.-Y., T.-H. Chu, and C.-L. Hu. 2013. Interrelated influence of light and Ni on *Trichodesmium* growth. *Front. Microbiol.* **4**: 139. doi:10.3389/fmicb.2013.00139
- Ho, T.-Y., X. Pan, H.-H. Yang, G. T. F. Wong, and F.-K. Shiah. 2015. Controls on temporal and spatial variations of phytoplankton pigment distribution in the Northern South China Sea. *Deep-Sea Res. Part II Top. Stud. Oceanogr.* **117**: 65–85. doi:10.1016/j.dsr2.2015.05.015
- Karl, D. M., and others. 2002. Dinitrogen fixation in the world's oceans. *Biogeochemistry* **57/58**: 47–98. doi:10.1023/A:1015798105851
- Kumar, S., and H. Polasa. 1991. Influence of nickel and copper on photobiological hydrogen production and uptake in *Oscillatoria subbrevis* strain 111. *Proc. Indian Natl. Sci. Acad.* **57B**: 281–285.
- Luo, Y.-W., and others. 2012. Database of diazotrophs in global ocean: Abundance, biomass, and nitrogen fixation rates. *Earth Syst. Sci. Data* **4**: 47–73. doi:10.5194/essd-4-47-2012
- Mackey, D. J., J. E. O'Sullivan, R. J. Watson, and G. Dal Pont. 2002. Trace metals in the Western Pacific: Temporal and spatial variability in the concentrations of Cd, Cu, Mn and Ni. *Deep-Sea Res. Part I Oceanogr. Res. Pap.* **49**: 2241–2259. doi:10.1016/S0967-0637(02)00124-3
- Masukawa, H., M. Mochimaru, and H. Sakurai. 2002. Disruption of the uptake hydrogenase gene, but not of the bidirectional hydrogenase gene, leads to enhanced photobiological hydrogen production by the nitrogen-fixing cyanobacterium *Anabaena* sp. PCC 7120. *Appl. Microbiol. Biotechnol.* **58**: 618–624. doi:10.1007/s00253-002-0934-7
- Min, H., and L. A. Sherman. 2010. Hydrogen production by the unicellular, diazotrophic cyanobacterium *Cyanothecce* sp. strain ATCC 51142 under conditions of continuous light. *Appl. Environ. Microbiol.* **76**: 4293–4301. doi:10.1128/AEM.00146-10
- Moore, R. M., S. Punshon, C. Mahaffey, and D. Karl. 2009. The relationship between dissolved hydrogen and nitrogen fixation in ocean waters. *Deep-Sea Res. Part I Oceanogr. Res. Pap.* **56**: 1449–1458. doi:10.1016/j.dsr.2009.04.008
- Moore, R. M., M. Kienast, M. Fraser, J. J. Cullen, C. Deutsch, S. Dutkiewicz, M. J. Follows, and C. J. Somes. 2014. Extensive hydrogen supersaturations in the western South Atlantic Ocean suggest substantial underestimation of nitrogen fixation. *J. Geophys. Res. Oceans* **119**: 4340–4350. doi:10.1002/2014jc010017
- Moore, R. M., I. Grefe, J. Zorz, S. Shan, K. Thompson, J. Ratten, and J. LaRoche. 2018. On the relationship between hydrogen saturation in the tropical Atlantic Ocean and nitrogen fixation by the symbiotic diazotroph UCYN-A. *J. Geophys. Res. Oceans* **123**: 2353–2362. doi:10.1002/2017jc013047
- Price, N. M., G. I. Harrison, J. G. Hering, R. J. Hudson, P. M. V. Nirel, B. Palenik, and F. M. M. Morel. 1989. Preparation and chemistry of the artificial algal culture medium Aquil. *Biol. Oceanogr.* **6**: 443–461. doi:10.1080/01965581.1988.10749544
- Punshon, S., and R. M. Moore. 2008. Aerobic hydrogen production and dinitrogen fixation in the marine cyanobacterium *Trichodesmium erythraeum* IMS101. *Limnol. Oceanogr.* **53**: 2749–2753. doi:10.4319/lo.2008.53.6.2749
- Rodriguez, I. B., and T.-Y. Ho. 2014. Diel nitrogen fixation pattern of *Trichodesmium*: The interactive control of light and Ni. *Sci. Rep.* **4**: 4445. doi:10.1038/srep04445
- Saito, M. A., J. W. Moffett, and G. R. DiTullio. 2004. Cobalt and nickel in the Peru upwelling region: A major flux of labile cobalt utilized as a micronutrient. *Global Biogeochem. Cycles* **18**: GB4030. doi:10.1029/2003GB002216
- Schlitzer, R., and others. 2018. The GEOTRACES intermediate data product 2017. *Chem. Geol.* **493**: 210–223. doi:10.1016/j.chemgeo.2018.05.040
- Scranton, M. I. 1983. The role of the cyanobacterium *Oscillatoria (Trichodesmium) thiebautii* in the marine hydrogen cycle. *Mar. Ecol. Prog. Ser.* **11**: 79–87. doi:10.3354/meps011079
- Scranton, M. I. 1984. Hydrogen cycling in the waters near Bermuda: The role of the nitrogen fixer, *Oscillatoria thiebautii*. *Deep-Sea Res. Part A Oceanogr. Res. Pap.* **31**: 133–143. doi:10.1016/0198-0149(84)90020-7
- Scranton, M. I., P. C. Novelli, A. Michaels, S. G. Horrigan, and E. J. Carpenter. 1987. Hydrogen production and nitrogen fixation by *Oscillatoria thiebautii* during in situ incubations. *Limnol. Oceanogr.* **32**: 998–1006. doi:10.4319/lo.1987.32.4.0998
- Tamagnini, P., E. Leitão, P. Oliveira, D. Ferreira, F. Pinto, D. J. Harris, T. Heidorn, and P. Lindblad. 2007. Cyanobacterial hydrogenases: diversity, regulation and applications. *FEMS*

- Microbiol. Rev. **31**: 692–720. doi:[10.1111/j.1574-6976.2007.00085.x](https://doi.org/10.1111/j.1574-6976.2007.00085.x)
- Wang, B.-S., C.-P. Lee, and T.-Y. Ho. 2014. Trace metal determination in natural waters by automated solid phase extraction system and ICP-MS: The influence of low level Mg and Ca. *Talanta* **128**: 337–344. doi:[10.1016/j.talanta.2014.04.077](https://doi.org/10.1016/j.talanta.2014.04.077)
- Waterbury, J. B., and J. M. Willey. 1988. Isolation and growth of marine planktonic cyanobacteria. *Methods Enzymol.* **167**: 100–105. doi:[10.1016/0076-6879\(88\)67009-1](https://doi.org/10.1016/0076-6879(88)67009-1)
- Welsh, E. A., and others. 2008. The genome of *Cyanothece* 51142, a unicellular diazotrophic cyanobacterium important in the marine nitrogen cycle. *Proc. Natl. Acad. Sci. USA* **105**: 15094–15099. doi:[10.1073/pnas.0805418105](https://doi.org/10.1073/pnas.0805418105)
- Wilson, S. T., R. A. Foster, J. P. Zehr, and D. M. Karl. 2010a. Hydrogen production by *Trichodesmium erythraeum* *Cyanothece* sp. and *Crocospaera watsonii*. *Aquat. Microb. Ecol.* **59**: 197–206. doi:[10.3354/ame01407](https://doi.org/10.3354/ame01407)
- Wilson, S. T., S. Tozzi, R. A. Foster, I. Ilikchyan, Z. S. Kolber, J. P. Zehr, and D. M. Karl. 2010b. Hydrogen cycling by the unicellular marine diazotroph *Crocospaera watsonii* strain WH8501. *Appl. Environ. Microbiol.* **76**: 6797–6803. doi:[10.1128/AEM.01202-10](https://doi.org/10.1128/AEM.01202-10)
- Wilson, S. T., Z. S. Kolber, S. Tozzi, J. P. Zehr, and D. M. Karl. 2012. Nitrogen fixation, hydrogen cycling, and electron transport kinetics in *Trichodesmium erythraeum* (cyanobacteria) strain IMS101. *J. Phycol.* **48**: 595–606. doi:[10.1111/j.1529-8817.2012.01166.x](https://doi.org/10.1111/j.1529-8817.2012.01166.x)
- Wilson, S. T., D. A. del Valle, J. C. Robidart, J. P. Zehr, and D. M. Karl. 2013. Dissolved hydrogen and nitrogen fixation in the oligotrophic North Pacific Subtropical Gyre. *Environ. Microbiol. Rep.* **5**: 697–704. doi:[10.1111/1758-2229.12069](https://doi.org/10.1111/1758-2229.12069)
- Xiankong, Z., F. R. Tabita, and C. Van Baalen. 1984. Nickel control of hydrogen production and uptake in *Anabaena* spp. strains CA and 1F. *Microbiology* **130**: 1815–1818. doi:[10.1099/00221287-130-7-1815](https://doi.org/10.1099/00221287-130-7-1815)
- Zhang, X., D. M. Sherman, and L. A. Sherman. 2014. The uptake hydrogenase in the unicellular diazotrophic cyanobacterium *Cyanothece* sp. strain PCC 7822 protects nitrogenase from oxygen toxicity. *J. Bacteriol.* **196**: 840–849. doi:[10.1128/JB.01248-13](https://doi.org/10.1128/JB.01248-13)

Acknowledgments

We thank Wan-Yen Cheng, Jie-Cheng Chang, Chih-Chiang Hsieh, and Wan-Chen Tu for providing technical support. This study was financially supported by grant MOST 105-2119-M-001-039-MY3 by Taiwan Ministry of Science and Technology and Career Development Award CDA-104-M11 by Academia Sinica.

Conflict of Interest

None declared.

Submitted 12 February 2019

Revised 12 June 2019

Accepted 25 July 2019

Associate editor: James Moffett